INTENSITY DEPENDENCE OF THE PHOTOVOLTAIC PARAMETERS OF ORGANIC BULK-HETEROJUNCTION SOLAR CELL

By

Bereket Gebre

A THESIS PRESENTED TO

THE SCHOOL OF GRADUATE STUDIES
ADDIS ABABA UNIVERSITY

IN PARTIAL FULFILLMENT OF THE REQUIREMENTS
FOR THE DEGREE

MASTER OF SCIENCE in PHYSICS

ADDIS ABABA, ETHIOPIA

MAY 2007

ADDIS ABABA UNIVERSITY

SCHOOL OF GRADUATE STUDIES

INTENSITY DEPENDENCE OF THE PHOTOVOLTAIC PARAMETERS OF ORGANIC BULK-HETEROJUNCTION SOLAR CELL

By

Bereket Gebre

Deaprment of Physics

Addis Ababa University

Approved by the Examining Board:

Dr. Genene Tessema Advisor _____

A.V. Gholap (Professor) Examiner _____

Dr. Tesgera Bedassa Examiner _____

Dated: May 2007

This Work is Dedicated to
TSION GEBRE

Table of Contents

List of Tables

List of Figures

Acknowledgements

I have a very high gratitude to my advisor, Dr. Genene Tessema for his excellent guidance, encouragement, and unlimited support during the time of the whole period of this work. Besides, his advices on how to create a conducive environment when working with colleagues were very special. I am also quite grateful to my parents for their financial and moral support.

A special thanks go to my friends. I am very lucky having friends like you who made my life easier and enjoyable. I also thank Teshale L. who has contributed directly or indirectly in the make up of this thesis.

Finally, I wish to express my gratitude to the Department of physics, Addis Ababa University.

Addis Ababa University Bereket Gebre

March, 2007

Abstract

As the evidence of global warming continues to build up, it is becoming clear that we will have to find ways to produce electricity with out the release of carbondioxide and other green house gases. Fortunately, we have renewable energy sources which neither run out nor have any significant harmful effects on our environment. Harvesting energy directly from the sunlight using photovoltaic (PV) technology is being widely recognized as an essential component of future global energy production. In this thesis, intensity dependence and a brief over view regarding photovoltaic properties of polymer based bulk heterojunction solar cell is presented and discussed.

Chapter 1

Introduction

Due to high population growth and economic development, the world's energy demand is at a very crucial stage. Most of the world energy needs today are met by fossil fuels such as oil, coal and gas. But, these are non-renewable, limited and unevenly distributed resources which could be exhausted in the future. So, continued increases in energy costs and strained demand on the oil reserves are spurring development of new technologies to meet global energy needs.

Hence, a world wide research is being conducted on solar cells that can be produced at low cost and still providing high conversion efficiencies. Polymer solar cells in which organic molecules with semiconductor properties absorb light and generate electrical power have emerged as a viable candidate from these efforts[1].

Conjugated polymers or polymers with alternating single and double carbon bonds, have been a subject of great interest in the development of solar cells[2]. At present, the best polymer solar cells are those based on a mixture of conjugated polymers and fullerenes (C_{60}). These devices provide power conversion efficiencies of $4-5\%$ in solar light, which is still less than the silicon solar cells[1].

In this thesis work we studied the electrical properties of junction between Aluminium and Poly[2-methoxy-5-(3',7'-dimethyloctyloxy)-1,4-phenylene vinylene] and MDMO-PPV blended with Phenyl-C_{61}-butyric acid methyl ester (PCBM) . We

used sandwich like structure of the form Al | MDMO−PPV | ITO and Al | MDMO−PPV | PCBM | ITO.

The first structure is used to compare the absorption spectrum of a single layer with a blend and see how the absorption band width increases for the blend structures. Also, it helps to know the wave length at which a maximum absorption took place. But, the second sandwich structure is used to investigate the light intensity dependence of the short circuit current and the open circuit voltage as well as to determine the current-voltage characteristics.

In the I-V characteristics measurement, we tried to see how the short circuit current (Isc) and the open circuit voltage vary with the variation of the incoming light intensity at a constant bias voltage. Then at a specific light intensity we tried to determine the impedance spectroscopy and the parameters that are attributed with a solar cell.

The second chapter deals with conjugated polymers. Bonding and the effect of doping in creating the quasi-particle as well as charge transport mechanism are discussed. The third chapter encompasses the basic features when a metal makes contact with semiconductor having different work function. The fourth chapter reviews solar cells starting from device architecture up to the basic working principles. Chapter five deals with the experimental part and the last chapter focuses on the discussion and conclusion based on the experimental result.

Chapter 2

Conjugated polymers

2.1 what are polymers?

Polymers are long range macromolecules, made from repeating monomeric units, with large molecular weight ($>$10000g/mole)[3]. Polymers have different properties. The chemical properties of polymers are the continuation of the behavior of the monomers that make up the polymers. Monomers are the smallest unit of the polymer that make up the polymer. In general, polymers have a structure H-$(CH_2)_n$-H and their physical property is determined by the number of -CH_2-groups, n could range from few hundred to several thousand.

Structurally, polymers can be classified in to linear chain (in which we find the functional group at each end in a straight line), networks (in which the functional groups are not aligned in a straight line as well as we have two reactive groups) and the third structure is the combination of the above structures

Another classification is based on the type of monomer. Polymers made from only one type of monomer units are called homopolymers, where as a copolymer contains structural units of two or more precursors[4].

Conjugated polymers are polymers with alternating single and double carbon bonds. This conjugation arises due to the polymer's ability to swap positions of

single and double bonds and end up with a structure that still satisfies the chemical bonding requirements.

When we compare the pi(π)-conjugated polymers with sigma (δ) bonded non-conjugated polymers, they have small band gaps, relatively large electron affinities and small ionization potentials[3].

Under normal conditions all conjugated polymers are either insulators or semiconductors with wide energy gap. They become conductors by the injection of electrons or holes on to the chains.

2.1.1 Chemical Bonding in conjugated Polymers

In order to understand the nature of physical and electrical properties of polymers one needs to know the structure of polymers. Most polymers are covalently bonded long chain macromolecules. The formation of a covalent bond involves sharing of two electrons, i.e the pair that can be accommodated in bonding molecular orbital.

Suppose two hydrogen atoms are brought together to form a molecule, the electrons of each atom in this case revolves around both nuclei forming a molecular orbital (MO). There are two ways in which the wave functions of the electrons in both hydrogen atoms superpose. One of these MOs is significantly lower energy than the sum of the energy of the original atomic orbital. It is known as bonding molecular orbital. The other orbital called anti-bonding MO is of higher energy than the original atomic orbital. Energetically the former gives a stable hydrogen molecule while the latter needs an expenditure of external energy[5,6].

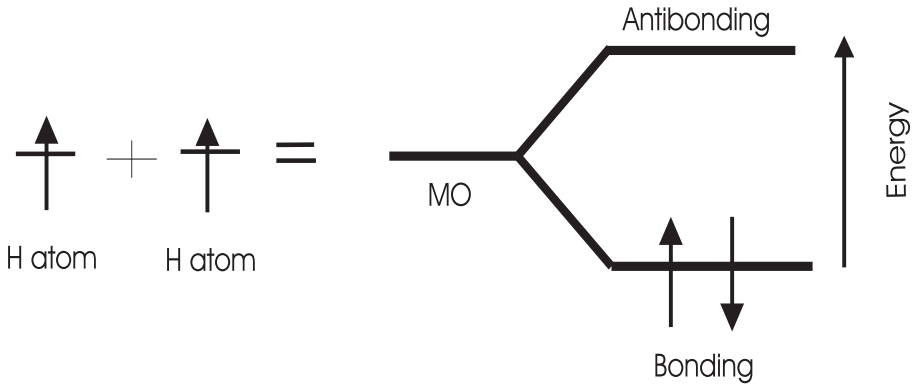

Figure 2.1: Molecular energy levels of a covalent bond in polymer

2.1.2 Pi (π) and Sigma (σ) bonds

When two electrons in covalent bond are shared in region of space common to the bonding atoms, the region of space is pictured as an overlap of two atomic orbital.

Figure 2.2: Cylindrically symmetric σ-bond of the hydrogen molecule MO

Such a bond that is cylindrically symmetrical around an axis joining the two nuclei is called sigma(σ)bond. The other bond is pi(π) bond that is formed by sideways overlap of parallel p-orbital[7]. (see figure 2.3).

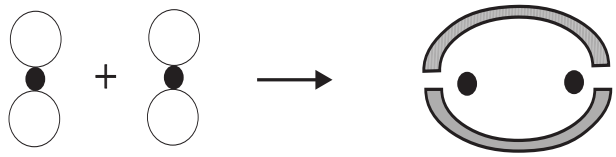

Figure 2.3: Two Molecular energy orbital overlap in covalent bond to form π-MO

2.1.3 Hybridization

Conjugated polymers are different from conventional polymers in such a way that the carbon atoms are hybridized either in SP-or SP^2 hybridization. But, in conventional polymers the carbon atoms are hybridized in the form of SP^3, this is because of the fact that carbon atom has four valence electron which can be shared by four neighboring atoms to form four covalent bonds. So, this bond is a sigma bond in which case the electrons are strongly localized and hence they don't contribute to the electric conduction.

Whereas in SP^2 hybridization, the carbon atom doesn't employ its 2s and 2p orbital. Instead,to give more stable covalent bonds, the 2s and two of the three P-electron ($2p_x$ and $2p_y$) of the carbon atom are combined to form three σ-bond with three neighbors resulting planar trigonal shaped structure. The remaining $2p_z$ orbital not participating in the bonding is located perpendicular to the plane containing three σ-bonds. When the $2p_z$ orbital of two adjacent atoms overlap sideways they combine into two molecular orbital.

Electrons in the π-bond aren't concentrated along an axis between the two atoms but are shared in regions of space above and below the plane defined by the SP^2 orbital. The π- electrons are the basis for the alternation of shorter (double) and longer (single) bonds. And these delocalized electrons are responsible for the conductivity in CPs.

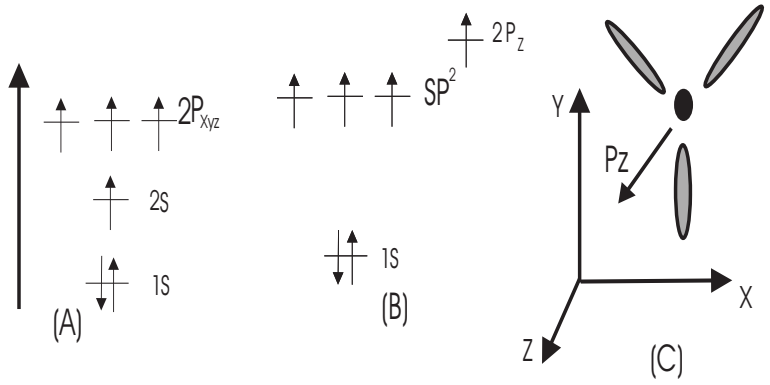

Figure 2.4: (a) Electronic configuration of the carbon atom, (b) The SP^2 hybridization with promoted 2S and (c) The atomic structure on XY plane

2.2 Quasi-particles

In inorganic semiconductor crystals such as silicon and Germanium the strong coupling between the atoms and long range order lead to the delocalization of electronic states and the formation of allowed valence and conduction bands separated by forbidden energy gap. By thermal activation or photo-excitation free electrons are generated in the conduction band, leaving behind positively charged holes in the valence band.

But, this is not the case in conjugated polymers. There are elementary excitations namely solitons, polarons, and bipolarons. These quasi particles are created mainly due to a process known as doping.

2.2.1 Doping of conjugated polymers

The change of electrical properties observed by the doping of polyacetylene in 1977 opened the door to research on conducting polymers (CPs). By doping conjugated polymers previously called semi conducting polymers, their conductivity increased by more than 10 orders of magnitude. It is fully recognized that doping is the

central process that governs the main properties of conjugated polymers, in particular the cross over to the conducting state. In a very general sense, any manner of changing the number of pi electrons (addition or withdrawal) can be called doping and gives rise to an increased conductivity[7].

Conjugated polymers properties can be changed drastically by doping. For example, the room temperature conductivity of polyacetylene changes from $10^{-3} - 10^{-5}\frac{S}{cm}$ to greater than $10^{5}\frac{S}{cm}$ upon doping with iodine; a value close to the conductivity of copper($5 \times 10^{5}\frac{S}{cm}$)[3].

Doping can be done in many ways. But the main doping mechanism is doping by chemical means. In chemical doping normally oxidizing or reducing process will take place via the interaction of the polymer with either oxidizing or reducing agent. Chemical doping can be accomplished by the exposure of the polymer to a solution or vapor of the dopant. Oxidizing agents such as iodine, arsenic pentaflouride (AsF_5), and sodium naphtalide. The main criterion for selecting oxidizing or reducing agent is their ability to oxidize or reduce the polymer without lowering its stability to conduct electricity as well as initiating side reaction that inhibits the conductivity of the polymers[6].

2.2.2 Creation of Quasi-particles upon doping and structural distortions

Polarons, Bipolarons and Solitons

Often in conducting polymers, one encounters the three quasi-particles namely; solitons, polarons and bipolarons. When we compare the energy of the excited state to that of the ground state, the energy of the excited state can be expressed as the sum of the excitation energies of those quasi-particles. Below this let us discuss the characteristics of those quasi-particles.

Solitons

Actually solitons can be generated in two ways. Intrinsically formed solitons

during synthesis and doping -induced solitons.

Consider two degenerate ground states of Trans-polyacetylene (fig4). Both phases have exactly the same energy, and they are idealized in such a way that there are no kinks or misfits appearing.

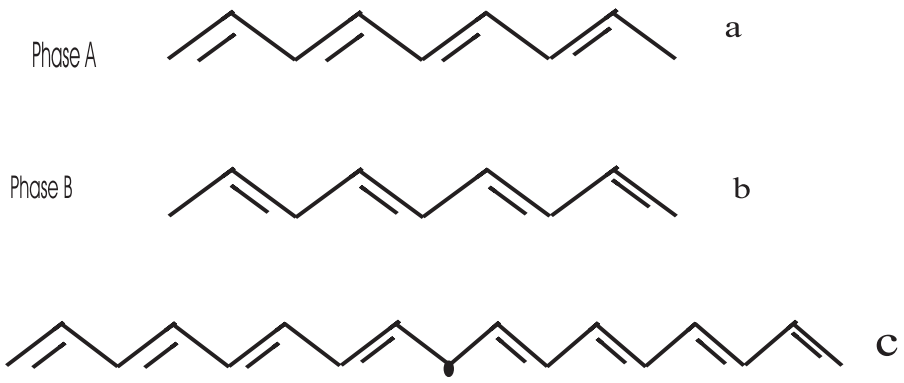

Figure 2.5: (a) and (b) stand for the ground state degeneracy of two phases of dimerized trans-polyacetylene (c) soliton separating the two phases of trans-polyacetylene chain

Now, let us imagine that the undimerized polacetylene chain undergoes dimerization i.e from disorder to order (peirl's) transition. Assume the dimerization starts simultaneously at both ends of the polymer chain and it propagates to the center. When the two phases meet, there is 50% probability of a misfit (a region in which two single bonds meet), refer to the above graph. This misfit separates the polymer into two domains. These domains are conjugation defects known as "solitons"

At the misfits, the atomic orbital don't know whether they should form bonding (π) or antibonding (π^*) states. Instead they form non-bonding states in the energy band gap and because of symmetry reasons they form a mid gap state.

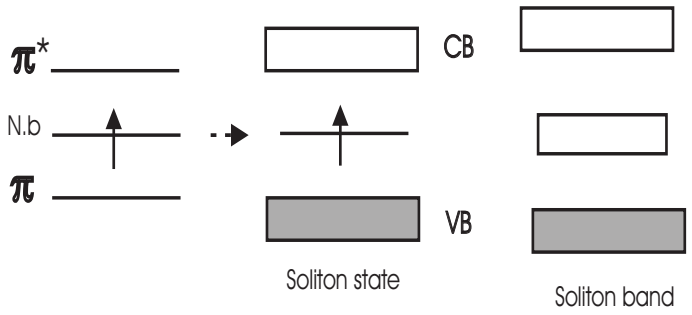

Figure 2.6: Formation of a mid-gap state due to the creation of soliton

Doping of conjugated polymers is a chemical redox reaction. As a result of charge transfer, there are three possible solitonic charges, namely charge ± 1 and 0.

Polyacetylene, for example can be oxidized with iodine (p-doping) or reduced (n-doping) with potassium.

$[CH]_x^0 + 3I_2 \rightarrow [CH]_x^{++} + 2I_3^-$ P-doping

$[CH]_x^0 + K^0 \rightarrow [CH]_x^- + K^+$ n-doping

Generally soliton formation results in the creation of new localized electronic state that appears in the middle of the energy gap. How ever at high doping levels, the charged solitons interact with each other to form a soliton band, which eventually merge with the band edges to create true metallic conductivity[5,6].

Polarons and **Bipolarons**

A polymer may store charge in two ways. In an oxidation process it could either lose an electron from one of the bands or it could localize the charge over a small section of the chain. Localizing the charge causes a local distortion due to a change in geometry, which costs the polymer some energy. How ever the generation of this local geometry decreases the ionization energy of the polymer chain and increases its electron affinity making it more able to accommodate the newly formed charges. This method increases the energy of the polymer less than

it would if the charge was delocalized and hence it takes place in preference of charge delocalization. A similar scenario occurs for a reductive process.

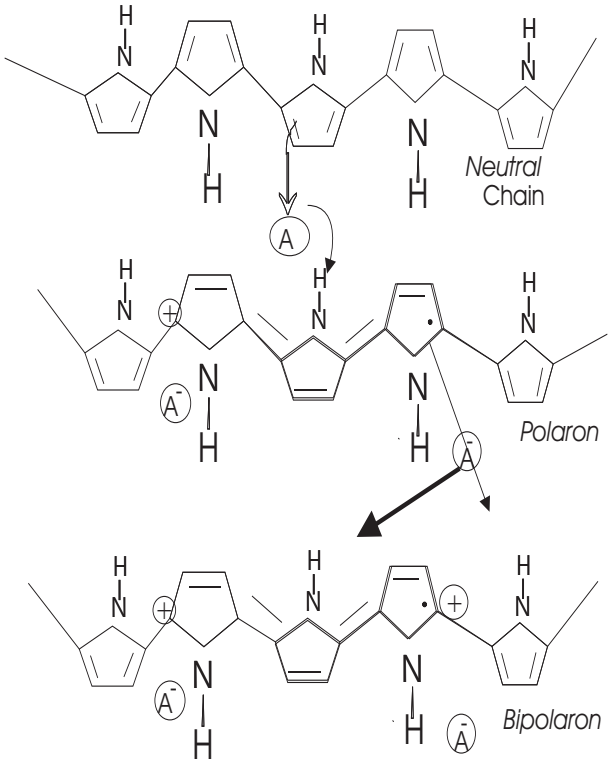

Figure 2.7: Formation of polarons and bipolarons

The oxidative doping of polypyrrole is carried out in the following way. An electron is removed from the P- system of the backbone chain producing free radical and spinless positive charge. The radical and cation are coupled to each other via local resonance of the charge and the radical. This combination of a charge site and a radical is called a polaron. This could be either a radical cation or radical anion. This creates a new localized electronic states in the gap, with the lower energy states being occupied by a single unpaired electron. The polaron state of polypyrrole are symmetrically located about 0.5eV from the band edges.

Upon further oxidation, the free radical of the polaron is removed, which

creates a new spinless defect called a bi-polaron. Bi-polaron formation requires lower energy than the creation of two distinct polarons. At higher doping levels it becomes possible that two polarons combine to form a bipolaron. Thus at higher doping levels the polarons are replaced with bipolarons. The bipolarons are located symmetrically with a band gap of 0.75eV for polypyrrole. Upon continued doping it eventually forms continuous bipolaron bands. For a very highly doped polymer it is conceivable that the upper and lower bipolaron bands will merge with the conduction the valence bands respectively so that it produces partially filled bands and create true metallic conductivity. This is shown below[8].

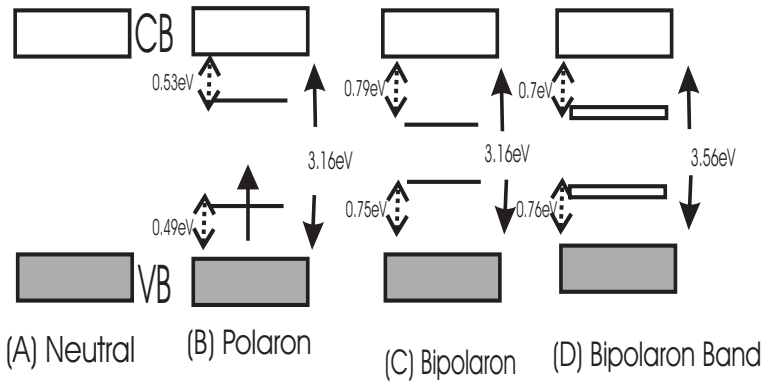

Figure 2.8: Formation of bipolaron bands

2.3 Charge Transport Mechanism

Most polymers are insulators. There are some polymers, however which become electrically conducting, by doping with strong oxidizing or reducing agents. This is because doping introduces more charge carriers than impurity concentration which leads to a reduced probability of recombination of electron-hole pairs.

Doping is the main process which affects the conductivity of polymers to a great extent. The dopant concentration is given in mol % taking one CH unit as a mole. So, scientists noted that upon increasing the doping level, the conductivity rises by many orders of magnitude, but, there is no sharp transition from an insulating to a metallic state[9].

Besides doping conductivity highly depends on the temperature. For metals conductivity increases with decreasing temperature. This is because of the fact that lattice vibrations freeze out as the temperature decreases to absolute zero. While in inorganic semiconductors, conductivity decreases drastically with decreasing temperature. It plays a major role in exciting the electrons from the valence band to the conduction band and hence the conductivity of inorganic semiconductors is greatly affected by temperature. But, the conductivity of doped conjugated polymers decreases if the temperature decreases, but slower than exponentially.

The effect of temperature on the conductivity is analyzed based on the doping level. For highly doped samples, the conductivity varies only slightly with the temperature, where as for low doping levels the temperature dependence is very drastic. Most highly doped samples behave like very dirty metals in which the conductivity is nearly temperature independent. In the case of dirty metals, the main obstacles to charge carrier motion are impurities and lattice defects. Since their concentrations are independent of the sample temperature, the conductivity becomes nearly constant with temperature[5].

In amorphous semiconductors conduction by free charge carriers isn't possible

because, the free electrons become localized and can only move by hopping (phonon-assisted quantum tunnelling) between localized states located in the forbidden gap. This fact applies to undoped or lightly doped conjugated polymers in order to understand the charge transport mechanism between localized solitonic, polaronic, and bipolaronic states. This process is known as variable range hopping (VRH). VRH is a thermally agitated process in which the conduction mechanism is dominated by electron hopping near the Fermi-level[10].

According to the VRH model, the temperature dependence of conductivity is given by

$$\sigma=\sigma_0 exp[-(\frac{T_0}{T})^{\gamma}]$$

Where, σ_0 and T_0 are fitting parameters and this formula is formulated by Mott[11] , in which case γ is related with the dimensionality and is given by

$$\gamma=\frac{1}{1+d}$$

So in three dimensional hopping d=3 and $\gamma=\frac{1}{4}$ and hence $\sigma=\sigma_0 exp[-(\frac{T_0}{T})^{\frac{1}{4}}]$

Chapter 3

Metal-Semiconductor contacts

Because of their importance in direct current and microwave applications and as tools in the analysis of other fundamental physical parameters, metal-semiconductor contacts have been studied extensively.

When a semiconductor of a given electrochemical potential is brought in contact with a metal having different electrochemical potential, charge will flow across the interface. The magnitude and the direction of this initial charge transfer will determine the electrical properties of the device. Charges will flow until the Fermi-levels in the two materials become coincident due to thermal equilibrium.

Depending on the relative magnitudes of the work functions of the metal and the semiconductor, the energy band edges of the semiconductor bend near the interface. The work function is the energy difference between the vacuum level and the Fermi-level. This quantity is denoted by $q\phi_m$ and equal to $q(\chi + V_n)$ in the semiconductor, where $q\chi$ is the electron affinity measured from the bottom of the conduction band Ec to the vacuum level, and qV_n is the energy difference between Ec and the Fermi-level.

In this thesis, we shall see the two basic contacts, namely rectifying and ohmic contacts. In most cases, rectifying contacts are made on n-type semiconductors. Consider the case $\phi_m > \phi_s$, the ideal thermal-equilibrium metal-semiconductor

energy band diagram is schematically given in Fig.3.1. Before contact, the Fermi-level in the semiconductor was above that in the metal. In order for the the Fermi-level to become a constant through the system in the thermal equilibrium, electrons from the semiconductor flow into the lower energy states in the metal, positively charged atoms remain in the semiconductor creating a space charge region.

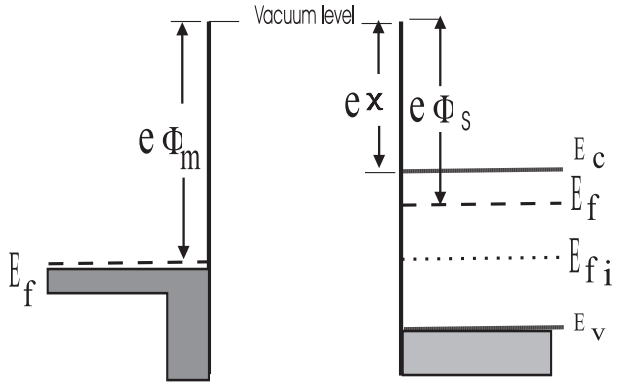

Figure 3.1: Energy band diagram of a metal and a semiconductor before contact

The parameter ϕ_{Bn} is the barrier height of the semiconductor contact, the potential barrier seen by electrons in the metal trying to move in to the semiconductor. The barrier is Known as the Schottky barrier and is given ideally by $\phi_{Bn}=(\phi_m - \chi)$ On the semiconductor side, V_{bi} the built-in potential barrier, the barrier seen by electrons in the CB trying to move into the metal. The built in potential barrier is given by $V_{bi}=(\phi_{Bn} - \phi_n)$[12].

If a positive voltage is applied to the metal with respect to the semiconductor, the built-in potential (V_{bi}) is reduced while ϕ_{Bn} remains constant. And hence electrons can move easily from the semiconductor into the metal. But motion of electrons will be blocked if a reverse bias voltage is applied. These kinds of contacts which allow the passage of electrons for only one type of bias are known as rectifying contacts.

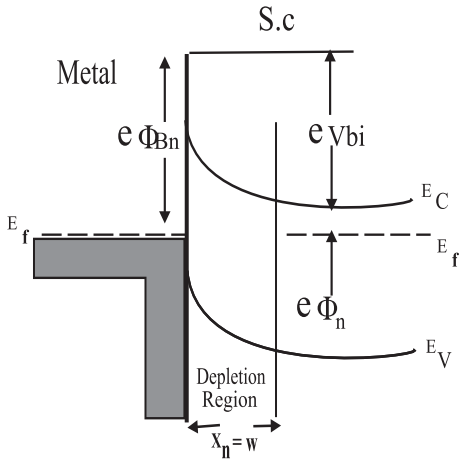

Figure 3.2: Ideal energy-band diagram of a metal and n-type semiconductor junction for $\phi_m > \phi_s$

Figure 3.3 shows the same ideal contact for opposite case of $\phi_m < \phi_s$. To achieve thermal equilibrium in this junction, electrons will flow from the metal in to the lower energy states in the semiconductor, which makes the surface of the semiconductor n-type.

If a positive voltage is applied to the metal, there is no barrier to electrons flowing from the semiconductor into the metal. If a positive voltage is applied to the semiconductor, the effective barrier height for electrons flowing from the metal to the semiconductor will be approximately $\phi_{Bn} = \phi_n$, so electrons can easily flow from the metal into the semiconductor. see Fig.3.4

These kinds of contacts which allow the passage of electrons for both types of bias voltages are known as Ohmic contacts.

The same process happens when a P-type semiconductor makes contact with a metal, but, the charge carriers in this case are holes. For a high work function metal and a P-type semiconductor interface the barrier is so low that charge carriers (holes) can readily pass across the junction. The contact is ohmic. see fig.3.5 left. On the right of this figure a schematic diagram of band bending is shown for a

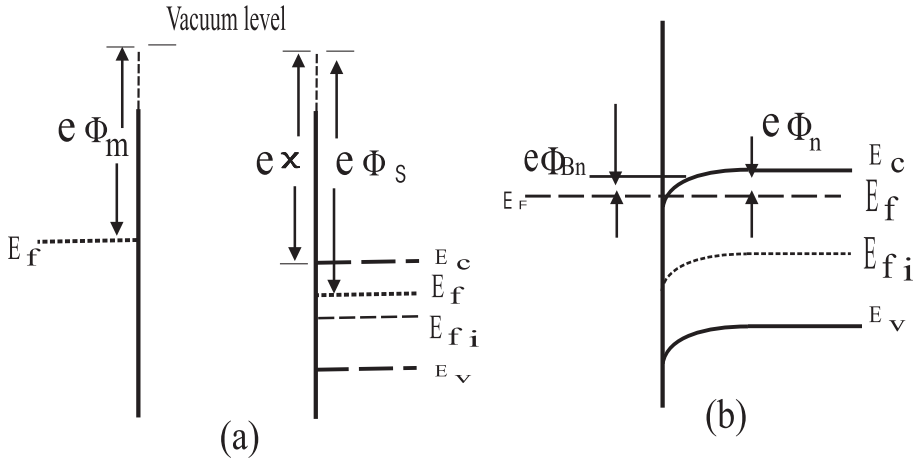

Figure 3.3: Ideal energy-band diagram (a) before contact (b) after contact for a metal-n-semiconductor junction for $\phi_m < \phi_s$

low work function metal and P-type polymer contacts. Such a junction has low resistance for holes flowing from the semiconducting polymer to the metal, and high resistance in the opposite direction.

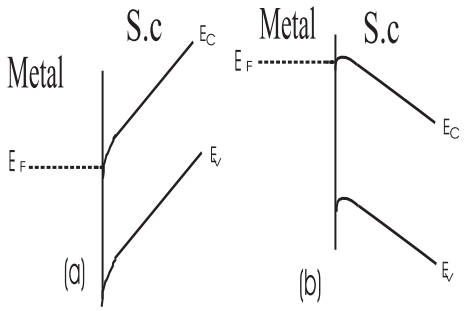

Figure 3.4: Ideal energy-band diagram of a metal n-semiconductor ohmic contact(a) with a positive applied voltage to the metal and (b) with a positive voltage applied to the semiconductor

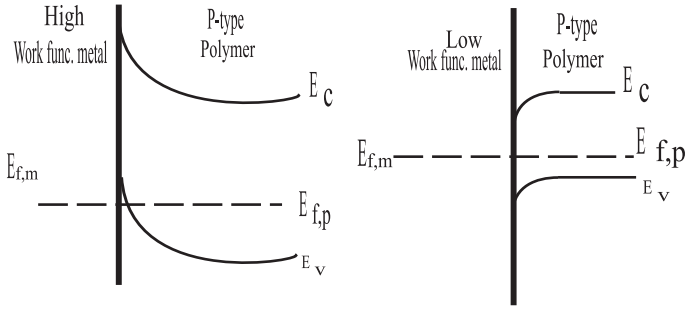

Figure 3.5: Band bending at the junction between a p- type semiconductor and a metal with high work function (left), and low work function(right)

3.1 Charge transport across metal-semiconductor contact

The transport in metal-semiconductor barrier is due to a majority charge carriers in contrast to a p-n junction where the minority carriers are responsible. The following figure shows the four basic transport processes under bias voltages.

The four processes are (1) transport of electrons from the semiconductor over

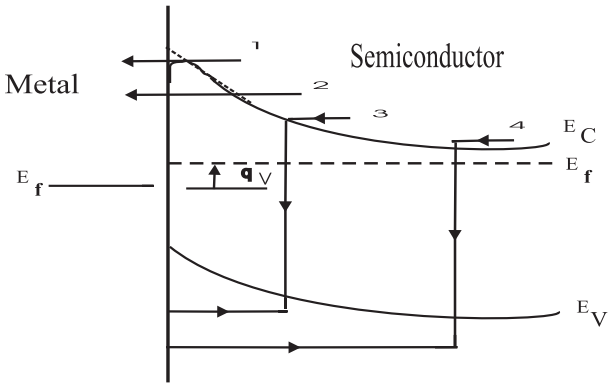

Figure 3.6: Four basic transport processes under forward bias

the potential barrier into the metal (common for Schottky diodes). (2) Quantum-mechanical tunnelling of electrons through the barrier(important for heavily doped semiconductor and responsible for most ohmic contacts), (3) Recombination in the space- charge region (4) Hole-injection from the metal to the semiconductor. In addition, we may have edge leakage current due to a high electric field at the metal - semiconductor interface[13].

Across the metal semiconductor interface there are two causes for the charge transport. One is the motion of the charges due to the external field or potential called drift current, the other one is diffusion current due to the difference in carrier concentration. In the case of drift, the applied voltage determines the way and magnitude of charge transfer.

The basic process in rectifying contact is by transport of electrons over the potential barrier which can be described by the thermionic emission theory. The thermionic emission characteristics are derived using the assumptions that the barrier height is much larger than kT, so that Maxwell-Boltzman approximation applies, and the thermal equilibrium is not affected by this process. The current represented in number one in the above figure represents the electron current density due to the flow electrons from the semiconductor into the metal. This

current density is a function of the concentration of electrons which have certain velocities sufficient to overcome the barrier. With the full derivation of the thermionic emission theory, one can find that, for many rectifying semiconductor-metal contacts, the voltage-current properties[13] can be described by

$$J = J_O[exp(\frac{qv}{nkt}) - 1]$$

Where

J is the total current density,

Jo is is the value of the reverse saturation current density,

q is the charge on the electron,

V is the applied voltage,

n is the diode ideality factor,

K is the Boltzman constant,

and T is the absolute temperature.

An important property of semiconductor contacts is the value of J_o. This will determine whether the junction acts as a rectifier, an ohmic contact, or a mixture of these limiting cases. From thermionic emission theory[13], the relation ship between the barrier height ϕ_b and J_o is given by

$$J_o = A^{**}T^2[exp(\frac{-q\phi_b}{KT})]$$

The exponential term represents the Boltzman factor relating fraction of the charges in the metal or semiconductor (at zero bias) which will overcome the barrier. The modified Richardson constant, A^{**}, expresses the number of electrons at the semiconductor-metal interface, which may be injected in to the metal. For organic semiconductor Schottky diodes the modified Richardson constant is assumed to be that of a free electron, namely, A^{**} =$120\frac{A}{cm^2k^2}$. Experimentally, J_o is obtained

by extrapolating the linear part of the plot of $\ln J$ V_s V and taking the intercept with the J axis. Then the value of ϕ_b is calculated using the above equation.

Case 1. If $Jo << J$, the contact will effectively block current flow for one sign of applied voltage (known as the reverse bias). This type of device will also display an exponentially increasing current when the bias voltage of opposite polarity (called the forward bias) is applied. Better rectification properties may be obtained for decreasing values of the reverse saturation current density, J_O[5].

Case 2. If $Jo >> J$, the contact will readily pass current for both signs of the applied voltage. So the exponential can be expanded to yield

$V = (\frac{nkt}{qJo})J$ which is linear and ohmic response displayed by the Metal-semiconductor contact system.

Case 3. If J_o is comparable to J, the J-V characteristics is non-ohmic and non-rectifying where the plot of J Vs V will show symmetric curve[14].

The above two equations obtained from the thermionic emission theory are used to characterize a solar sell in the next chapter.

3.2 Impedance Spectroscopy

Impedance Spectroscopy (IS) plays an important role in fundamental and applied electrochemistry and material science. In a number of respects, it is powerful method of characterizing many of the electrical properties of the interfaces of various substances with electronically conducting materials. It is also used in a medium that conducts ionically, electronically, electrons or holes or mixed electronic plus ionic conduction[15,16].

Impedance (Z) is generally defined as the total opposition a device offers to the flow of an alternating current (AC) at a given frequency, and is represented as a complex quantity which is graphically shown in a vector plane. The following figure shows the real part (resistance, R) and an imaginary part (reactance, X) of the impedance vector. The impedance vector can be represented using the rectangular

coordinate system as $R + jX$ or by the polar form using the magnitude and the phase angle θ.

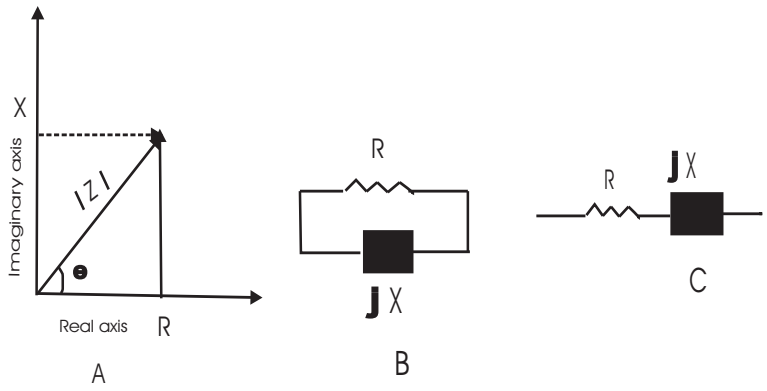

Figure 3.7: (a) Impedance complex plane (b) parallel (c) series connection of R and X

and hence,

$$Re(z) = R = \cos\theta$$

$$Im(Z) = X = \sin\theta = \sqrt{R^2 + X^2}$$

$$\theta = \tan^{-}\frac{X}{R}$$

The reciprocal of the impedance is known as the admittance and represented by Y. The whole expression then becomes $\frac{1}{Z} = \frac{1}{R+jX} = Y = G + jB$, where, G is known as the conductance and B is the susceptance.

The general approach in using impedance spectroscopy is by applying an electrical stimulus such as known voltage given by $V(t) = Vm(t)sin(\omega t)$, with a frequency $\omega = 2\pi f$, is applied to the device under test (DUT) and the resulting response of current $i(t) = Im(t)\sin(\omega t + \theta)$ is measured, where θ is the phase difference between the voltage and the current. $\theta = 0$ for pure resistors and $\theta = \frac{\pi}{2}$

for pure capacitors. Thus, a combination of a resistor and a capacitor in a network will have $0 < \theta < \frac{\pi}{2}$. The conventional impedance is defined as $Z(\omega) = \frac{V(t)}{i(t)}$, with $\theta = \theta(\omega)$. Impedance spectroscopy has been used to study the electrical and dielectric properties of polymers. Using this technique we are able to determine the resistance (R) and capacitance(C) of junction in the DUT.

The real and imaginary part of the impedance are recorded as a function of frequency and plotted on the complex plane. The real part is plotted along the X-axis and the negative of the imaginary along the Y-axis. Ideally the imaginary part of the impedance is zero at frequency, $\omega = 0$ and ω approaches ∞[25]. This plot forms a semi-circle with the center on the real axis. The very important idea in the modelling studies is much experimental results with the impedance of ideal resistor and capacitor equivalent circuits[17].

In circuit modelling, the resistance R represents the dissipative component of the electric response, a capacitance(C) describes the storage component of the electric material.

For instance consider RC connected in parallel. Keep in mind that the applied voltage and its response current is sinusoidal in nature with a frequency of $\omega = 2\pi f$, I is given by $I = \omega CVo(j\cos\omega t - \sin\omega t)$. Hence the total impedance of the circuit given in fig.3.8 (b)

$$Z = \frac{R}{1+jwRc}, \text{ the capacitive reactance is given by}$$

$$Xc = \frac{1}{jwc}, \text{ therfore,}$$

$Z = \frac{R}{1+\tau^2\omega^2} - j\frac{R\tau\omega}{1+\tau^2\omega^2}$ but, RC is defined as the relaxation time τ and hence,

$$Re(Z) = \frac{R}{1+\tau^2\omega^2}, -Im(Z) = \frac{R\tau\omega}{1+\tau^2\omega^2}$$

But, $\omega\tau = \frac{1}{\tan\theta}$, where θ is the phase difference between the voltage and the current. $\theta = 0$ for pure resistance and $\theta = \frac{\pi}{2}$ for pure capacitors, so in the network $0 < \theta < \frac{\pi}{2}$.

using the above relation we can write the real and imaginary parts of the impedance as

$$Re(Z) = R(1 - \cos^2\theta)$$

$$Im(Z) = R\cos\theta\sin\theta = \frac{-R}{2}\sin 2\theta$$

Based on the last relation, the imaginary component is maximum at $2\theta = \frac{\pi}{2}$, in which case $-IM(Z) = \frac{R}{2}$ and $\omega\tau = 1$. Then, the diameter of the semi-circle corresponds to R. The Cole-Cole plot of this circuit will be semi-circle whose center lies on the real axis of the impedance. If we add a resistor Rc in series to the above modelling, the impedance will be given by $Z = R_c + \frac{R}{1+j\omega c}$

The impedance across a metal-semiconductor contacts can be represented bya model that involves R, C and Rc. R and C represent the depletion region while Rc represents the contact resistance.

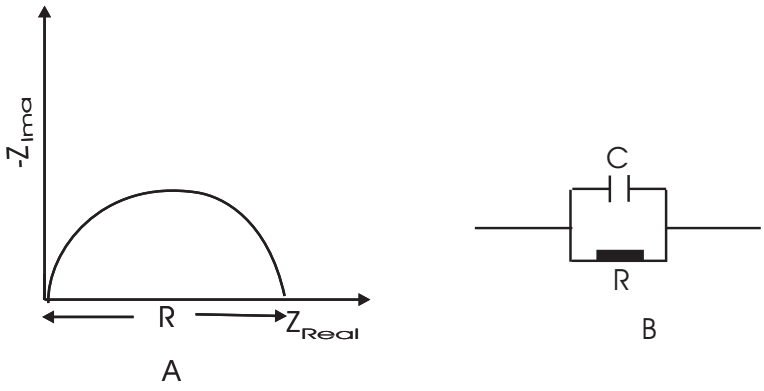

Figure 3.8: Representation of (a) Z of RC in complex plane and (b) RC in parallel circuit

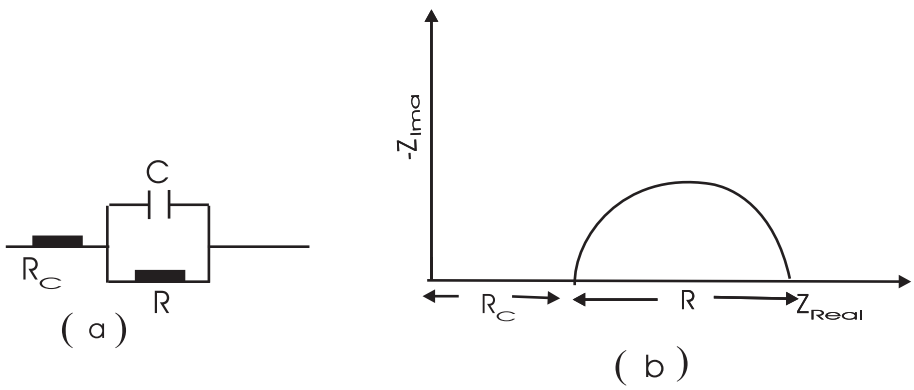

Figure 3.9: (a) Combination of resistors Rc, R and capacitor C, (b) Cole-Cole plot of impedance Z of the circuit

Chapter 4

Solar Cells: An over view

Introduction

More than any other Single factor, the increasingly recognized need to develop inexpensive and potentially renewable energy sources has caused a tremendous expansion of research efforts in photovoltaic. The economic appeal of being able to efficiently convert a free abundant supply of solar energy directly in to electricity is obvious.

There are three generations of development of photovoltaic. The first generation photovoltaic, consists of a large-area, single layer p-n junction diode, which is capable of generating usable electrical energy from light sources with the wavelengths of sunlight. These cells are typically made using a silicon wafer. First generation photovoltaic cells (also known as silicon wafer based solar cells) are the dominant technology in the commercial production of solar cells.

The second generation of photovoltaic materials is based on the use of thin film deposits of semiconductors. These devices were initially designed to be high efficiency, multiple junction photovoltaic cells. Later, the advantage of using a thin film of material was noted, reducing the mass of material required for cell design. This contributed to a prediction of greatly reduced costs for thin film solar cells. Typically, the efficiencies of thin film solar cells are lower compared with bulk

silicon solar cells.

The third generations of photovoltaic are very different than the other two, broadly defined as semiconductor devices which don't rely on traditional p.n junction to separate photo generated charge carriers. These new devices include photo electrochemical cells, polymer solar cells and nano crystal solar cells. This thesis deals with the polymer solar cells.

4.1 Device architecture

Light absorption in organic materials leads to the creation of excitons (electron-hole pair) that possess a strong binding energy. As the binding energy in organic semi-conductors is generally very large ($0.1 - 1$ev) compared to Silicon, the built-in electric fields are usually not high enough to dissociate the excitons directly. Hence, a process has to be introduced that efficiently separates the bound electron-hole pars. This is possible due to the sharp drop of potential at donor -accepter (D-A) as well as semiconductor-metal interfaces.

Depending on their efficient dissociation mechanisms of excitons into free charge carriers, we have three basic types of device architectures.

4.1.1 Single Layer Devices

Among the three types of devices, single layer devices are the simplest ones. The configuration of these devices is ITO | polymer | Aluminium. The ITO and the Aluminium are the electrodes, the ITO acting as an anode and the Aluminum acts as a cathode. Solar photons can enter the cell through the transparent contact(ITO) and create excitons upon absorption in the organic film. So at open circuit conditions holes are collected at high work function electrode(ITO), and electrons are collected at low work function electrode(Al). Indeed, the open circuit voltage(Voc) depends on the work function difference between the two electrodes. Consider the following figure.

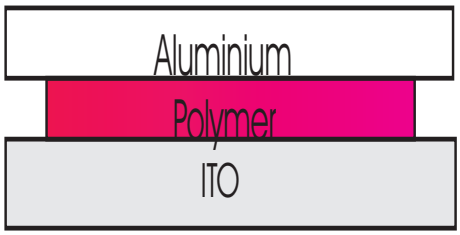

Figure 4.1: architecture of single layer device

In the above interface, excitons are formed via the absorption of a photon by the polymer. And hence in order to separate the created excitons into free charge carriers, there has to be an interface between materials of different electron affinity. In this case an interface between polymer | Aluminium and polymer | ITO. The excitons are dissociated into free charge carriers by the application of an electric field across the polymer layer. Photo- induced charges are selectively transported, assisted by the external field. Under forward bias electrons are injected from the Aluminium to the conduction band and holes from the ITO to the valence band. The efficiency of these devices is limited by short exciton diffusion length and high rate of recombination of free charge carriers due to the lack of having an immediate interface between the polymer and the electrode within the diffusion length.

4.1.2 Double Layer Devices

Compared to a single layer device this one is more efficient. In these bilayer devices the conjugated polymer is used as an electron donor and the organic molecule C_{60} as electron acceptor. The photo generated exciton moves towards the donor-acceptor interface and dissociates into free charge carriers. The mechanism involved in this process is that the highly electronegative C_{60} dissociates the excitons and accepts an electron. The exciton diffusion length in the active layer limits the performance of such a device like that of a single layered ones. The exciton diffusion length in a

conjugated polymer is~ 10nm.

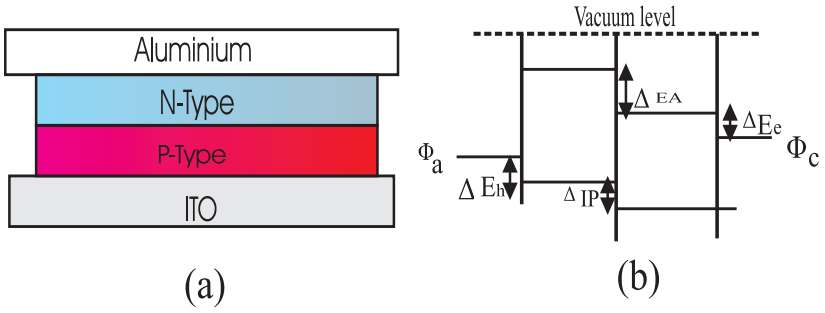

Figure 4.2: (a)architecture of double layer device (b) energy level of a bilayer device

So the thickness of such a device should be small enough inorder to make all the excitons reach the interface and be converted to free charge carriers. It is also to be noted that eventhough the charge transfer process at the interface happens within nanoseconds, the transport property of C_{60} is poor, which results in low transfer of free charge carriers to the electrodes. This increases the probability of recombination . A schematic diagram of the energy level of a bilayer device is shown above. Other than C_{60} , organic molecules and polymers with high electron affinity were used in such kind of structures.

4.1.3 Bulk Heterojunctions

Bulk heterojunctions active layer are produced by blending (mixtures of donor and acceptor materials) both n-type and p-type polymers in an appropriate solution and form the layer by spin coating. In this case, photo induced excitons are separated at the molecular level between the p-and n-type polymer. Since this ranges to the entire bulk of the polymer molecules, it drastically increases the current from such devices as compared to the other two structures.

The essence of bulk heterojunction is to intimately mix the donor and the acceptor components in a bulk volume so that each donor-acceptor interface is

within a distance less than the exciton diffusion length of each absorbing site. In figure 4.3, the situation is schematically shown for bulk heterojunctions. Bulk heterojunction exhibits an increased interfacial area where charge separation occurs.

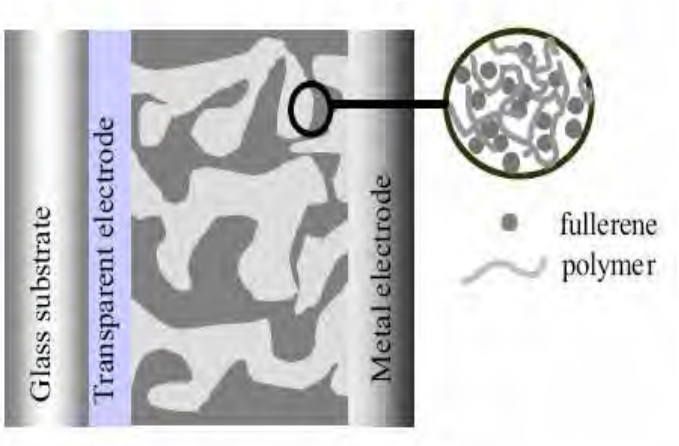

Figure 4.3: architecture of bulk heterojunction

Though in the bilayer heterojunction the donor and the acceptor phase contact the anode and the cathode selectively, the bulk heterojunctions require percolated pathways for the hole and electron transporting phases to the contacts[18,19]. In addition to this, blends require high solubility of both components.

4.2 Basic working principles

The process of converting light in to electric current in an organic photovoltaic cell is accomplished by the following consecutive steps.

The first step involves the absorption of a photon. When light of energy greater than the energy band gap is incident on the active area, it leads to the formation of an excited state , the electron -hole pair (exciton). n most organic devices a small portion of the incident light is absorbed due to large energy band gap, the organic layer and reflection losses are probably significant. This process is followed by the exciton diffusion. Ideally all photo-excited excitons should reach a dissociation site. Since such a site may be at the other end of the semiconductor, their diffusion length should be at least equal to the required layer thickness (for sufficient absorption). Other wise they recombine and photons are wasted.

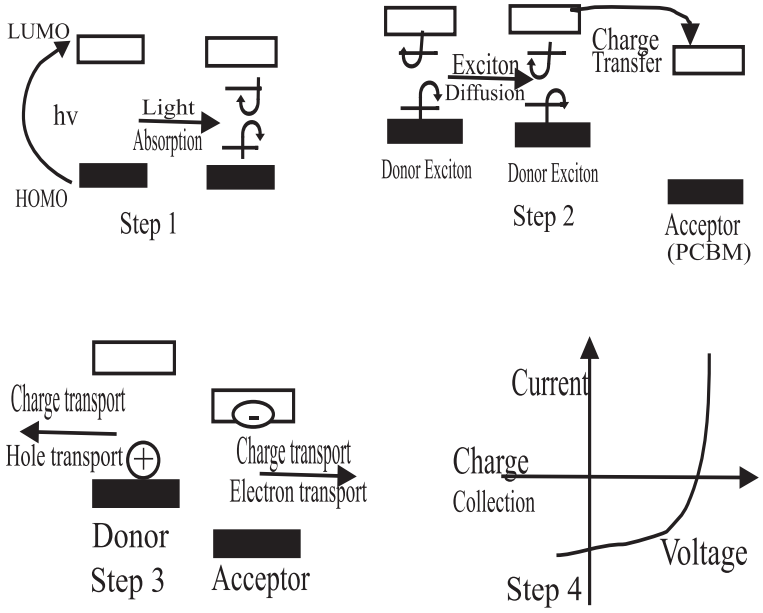

Figure 4.4: steps of current generation

In the next step, the diffused excitons should be separated into free charge

carriers. Charge separation is known to occur at organic semiconductor-metal interfaces, impurities (eg oxygen) or materials with sufficiently different electron affinities and ionization potentials. Once the excitons are separated into free charge carriers, they have to be transported to the respective electrodes. The transport of charges is affected by recombination during the journey to the electrodes, particularly if the same material serves as transport medium for both electrons and holes. Also, interaction with atoms or other charges may slow down the travel speed and there by limit the current. The last step involves charge collection. In order to enter an electrode material with a relatively low work function (eg Al,Ca) the charges often have to overcome the potential barrier of a thin oxide layer. In addition, the metal may have formed a blocking contact with the semiconductor so that they cannot immediately reach the metal[20]. The whole steps can be summarized in the above figure.

4.2.1 Characterization of the performance of a solar cell

The potential energy stored within one pair of separated positive and negative charges is equivalent to the difference in the electrochemical potential. Though for ohmic contacts no loss is expected, energy level offsets or band bending at non ohmic contacts (that under go energy-level alignments due to Fermi-level difference) can lead to a decrease in photo voltage. The electric current that a solar cell delivers corresponds to the number of created charges that are collected at the electrodes. This number depends on the ratio of photons absorbed to that of electron-hole pairs that are dissociated[21].

The following parameters are important in characterizing the performance of a solar cell.

1. Current density-Voltage (J-V) characteristics

   A typical J-V characteristics of a solar cell is depicted by the following figure.

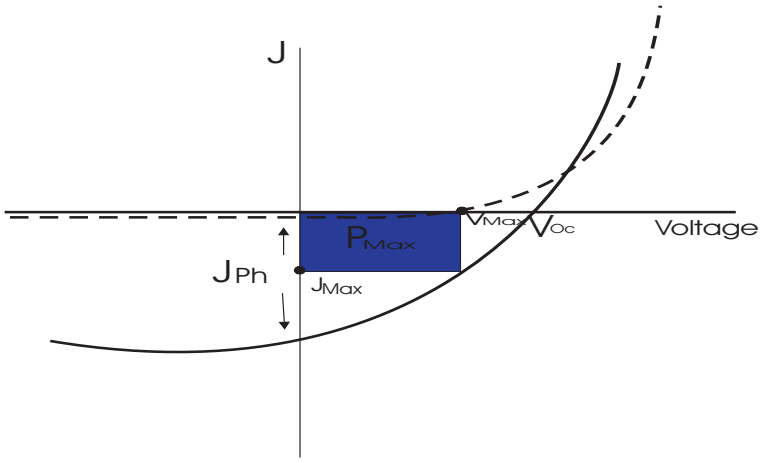

Figure 4.5: J-V characteristic under dark and illumination

When a solar cell is in darkness, current is increased exponentially with the application of a forward bias and almost blocked when a reverse bias is applied (dashed line in the figure). This is rectification property of a diode, often characterized by the rectification ratio, RR, given by the ratio of current densities between two applied voltages with opposite sign.

Under illumination (solid line), current flowing in the circuit is pure phot-induced current, namely short circuit current. It refers to the photo generated current of a solar cell which is extracted at zero applied voltage. Under illumination , the net observed equilibrium current density is given by

$$J = J_d - J_{ph} = J_o[\exp(\frac{eV}{nKT}) - 1] - J_{ph}$$

Where, J_d is the current density in the dark and, J_{ph} is the photocurrent

With increasing applied forward bias, the electric field-induced current (J_d) competes with the photo-induced current (J_{ph}) and at a certain applied voltage, the two

currents cancel each other. This voltage is known as the open circuit voltage, V_{oc}. In other words open circuit voltage of a solar cell is the voltage at which the net current J is equal to zero ($J_d = J_{ph}$). Mathematically it can be formulated as

$$V_{oc} = (\frac{nKT}{e}) \ln(1 + \frac{J_{ph}}{J_o})$$

For a J-V curve of a diode that is illuminated with light, the ratio of the maximum of the product of J_m and V_m to the product of J_{sc} and V_{oc}, is referred as the fill factor, FF. It is the measure of the power that can be extracted from the cell and can be put as

$$\mathbf{FF} = \frac{J_{max}.V_{max}}{J_{sc}.V_{oc}}$$

2. Power conversion efficiency (η)

This is the ultimate measure of the device efficiency in converting photons to electrons. It can be determined from the J-V characteristics and written as

$$\eta = \frac{P_{out}}{P_{in}} = \frac{J_m.V_m}{P_{in}} = \mathbf{FF}.\frac{J_{sc}.V_{oc}}{P_{in}}$$

Chapter 5

Experimental

5.1 Sample preparation

In this experiment, the active layer is prepared from the solution of polymers MDMO:PPV and PCBM in 1 : 4 weight ratio, at $10\frac{\mathrm{mg}}{\mathrm{ml}}$ of concentration. First 2 mg of MDMO;PPV, and 8 mg of PCBM were measured. Again two of them were mixed with a milliliter of chloroform which serves as a solvent. So for this purpose 1.47 g of chloroform is added to a container containing MDMO:PPV and PCBM powder.

5.2 Device Preparation

Commercially obtained ITO was cut to size of 2 by 1.5 cm. This is the exact size to be placed in the sample holder during measurements. In order to avoid ohmic contacts during measurements, some part of the ITO should be removed. About $\frac{2}{3}$ of the ITO glasses were covered by a photo resistive material and placed in a container containing a mixed hot solution of HCl, HNO_3 and H_2O in 48 : 4 : 48 ratio by volume respectively. This mixture of acids will remove the uncovered part of the ITO. The photo resistive material is detached and washed with water.

Furthermore, to avoid any remnants of the photo resistive material, the ITO-glass substrates were cleaned with acetone and rinsed with ethanol. Finally, the substrates are washed with distilled water and ready for the spin coating of the polymer.

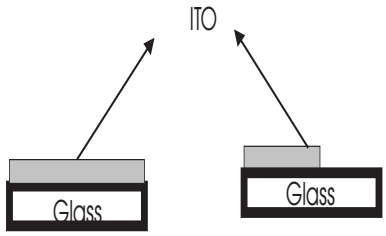

Figure 5.1: structure of ITO-glass substrate

First, partially etched glass substrates were cleaned and spin coated with a transparent, water soluble polymer known as Poly(3,4-ethlene dioxy thiophene) (PEDOT:PSS). This is done mainly for two purposes. PEDOT:PSS makes ohmic contact with most of P-type polymers as a result there will be an effective transportation of hole charge carriers. In this experiment, the ITO collects the holes enhanced by the PEDOT:PSS. The second use of PEDOT:PSS is, during etching of the ITO glasses, there are microscopic holes (not the charge carriers) that could affect the motion of the charge carriers. These holes will be filled with PEDOT:PSS and charges are collected at the respective electrode.

Since thin layer of PEDOT:PSS is needed, the speed of spin coating is 3000rpm which corresponds to 10nm thickness. After the water molecules are fully evaporated from the spin coated PEDOT:PSS, the active layer was spin coated at 1000rpm which corresponds to 100nm. Finally, the Aluminium electrode is deposited on top of the active layer using Edwards Auto 306 vacuum depositor.

Effective (active) area of the junction (the area under the contact of AL, Polymer and ITO of the device was about $4.5x10^{-2}cm^{-2}$. The sandwich structure shown above is a typical representative for current-voltage and complex-impedance

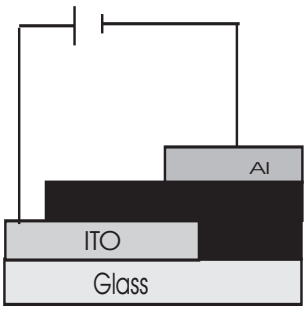

Figure 5.2: Structure of a sample ready for measurement

spectroscopy measurement.

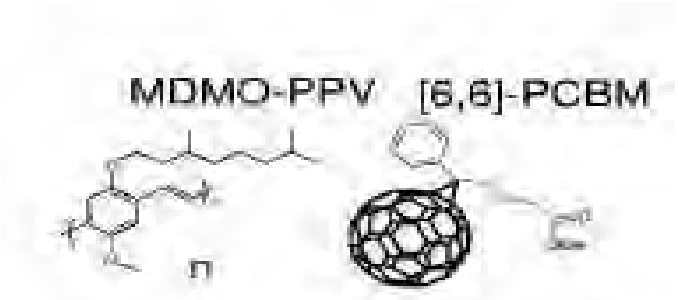

Figure 5.3: Chemical structure of MDMO-PPV and PCBM

5.3 Measurement Techniques

5.3.1 Absorption Measurement

The optical absorption of MDMO:PPV and MDMO:PPV | PCBM were taken after the solution of both samples was spin coated on transparent glass substrates. The absorption spectra were taken using PERKIN-ELMER UV | VIS | $NIR\lambda - 19$ spectrometry. The spectra can also be used to calculate the band gap of the polymer

based on the equation;

$$E_g = h\nu = \frac{hc}{\lambda}$$

Where $h = 6.625x10^{-34} J.Sec$ is planck's constant, c is the speed of light and λ is the wavelength at which the absorption has started. This measurement also helps to know the wavelength at which a maximum absorption took place.

5.3.2 Current-Voltage measurement

To determine the I-V characteristics of the device produced, HP 4140 B PA meter DC voltage source and HP 16055 A-TEST FIXTURE interfaced with computer were used. During measurement, the sample was placed at room temperature. The device under test (DUT) is connected in such a way that the applied voltage supports the motion of the charge carriers, i.e Al to negative terminal, while the ITO to the positive terminal. For I-V measurement under white light illumination, the bias voltage was scanned between $-2V to + 2V$ in steps of $0.05V$. For the dark measurement, the applied voltage was scanned between -3V and 3V in the same steps.

5.3.3 Impedance Measurement

Complex impedance spectroscopy of the sample was measured as a function of frequency and applied voltage using HP 4192 A LF Impedance Analyzer together with HP 10047-TEST FIXTURE. Frequency range of 10 kHz-100 kHz in steps of 2 kHz and bias voltages ± 2 and ± 1 V were used. The real and imaginary values of the impedance were recorded as a result a Cole-Cole plot drawn and discussed in the next chapter.

Chapter 6

Result and discussion

6.1 Absorption spectrum

The optical absorption of both MDMO:PPV and MDMO:PPV-PCBM is given in fig.6.1 and 6.2.

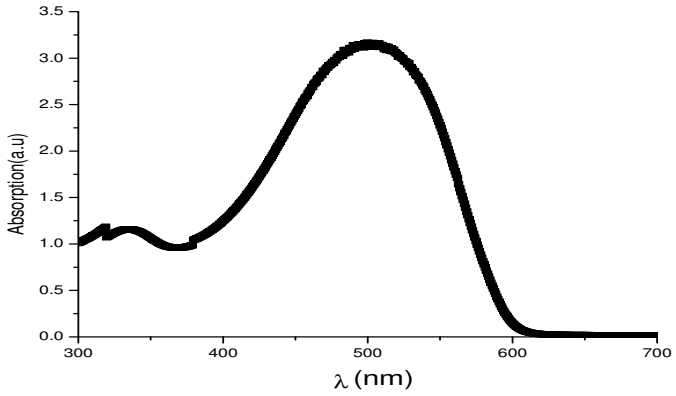

Figure 6.1: Absorption spectrum of MDMO:PPV

The figures indicate that absorption of electromagnetic radiation took place in the visible range. The absorption of pure MDMO:PPV shows absorption started

nearly at a wave length of 606nm. Using the relation $Eg = \frac{hc}{\lambda}$, the energy band gap of pure MDMO:PPV is determined to be 2 ev. Semiconductors are characterized by an energy band gap of $1.5 - 3ev$ as a result the above pure organic polymer falls into semiconductor category.

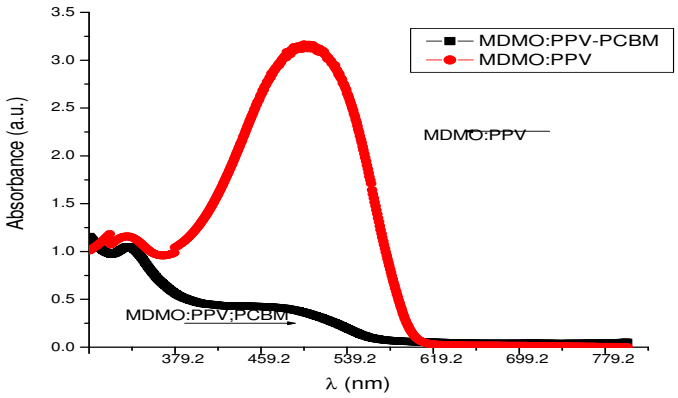

Figure 6.2: Absorption spectrum of MDMO:PPV and blend of MDMO:PPV with PCBM

In the polymer blend, it is observed that there is a widening of the absorption region as well as shift of a point where the absorption starts . As it can be seen from the figures there is a shift from 606 to 580 nm. But there is no significant change or shift between the peaks of pure MDMO:PPV and the polymer blend. In both samples maximum absorption took place at about 500 nm which corresponds to an energy of 2.5 eV. As it seen from the optical absorption spectrum, the sample covers only the visible range of the solar spectrum, less than 650nm. But, this will affect the efficiency of the device because a substantial solar energy is located in the red and infrared region[22].

6.2 J-V characteristics under dark

In order to understand the photovoltaic properties of the device, the J-V characteristics of the cell were studied. The J-V curve of Al |MDMO;PPV- PCBM | ITO sandwich structure in the dark is given in figure 6.3

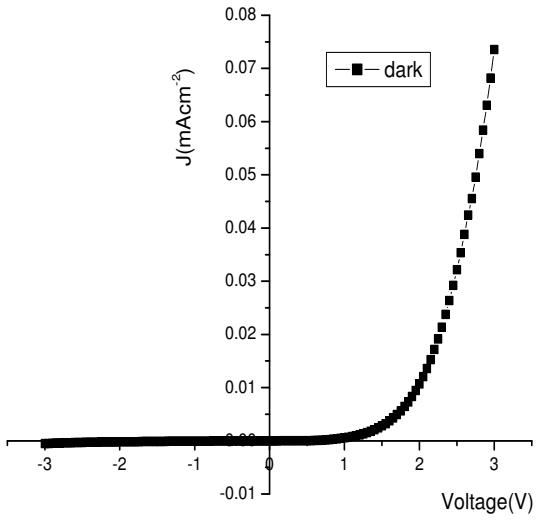

Figure 6.3: J-V characteristics under dark

As it is seen, the J-V curve of our sample in the dark is non-ohmic and asymmetric. At low or reverse bias voltages the current is almost blocked , but for forward bias voltages the current increases exponentially. This is due to the injection of charge carriers from the electrodes. This fact confirms that a schottky barrier rectifying contact is formed at the interface between Aluminium and the polymer. For the above J-V curve, the rectification ratio at$\pm 3V$ was determined to be about 157.

Again plot of $\ln(J)\nu_s V$ of the device under test revealed three main features. The first one is the low bias regime which is characterized by an ohmic flow

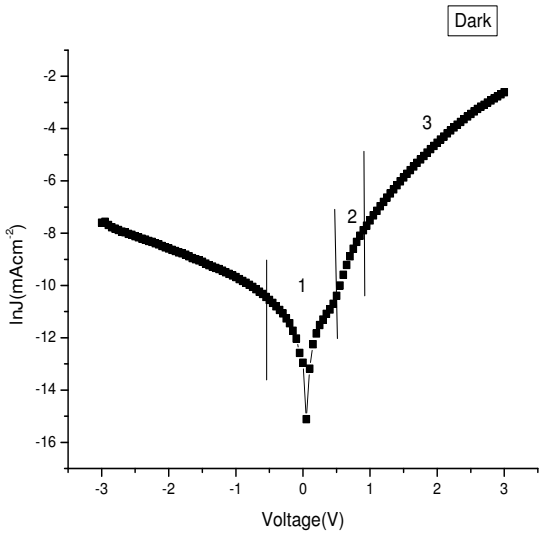

Figure 6.4: Semi logarithmic scale in dark

of charges. Due to the low bias voltage, the injection of charge carriers from the electrodes to the semiconductor material is small . The second region is found for intermediate values of bias voltages. This region is characterized by a sharp slope which shows injection-limited current and the current increases exponentially with bias voltage. The third regime corresponds to a high bias voltage values. It is characterized by flat band condition in which the built-in potential of the diode is compensated by the applied voltage. The effective barrier height is given by $V = V_{bi} \mp V_{app}$ (+ for the reverse bias and - for forward bias). V_{bi} is the built-in potential under thermal equilibrium when the Aluminium makes contact with the polymer. V_{app} is the applied voltage. So, at high forward bias voltage, the injection becomes enormous. The transport of charge flow is now dominantly controlled by the space charge limited current resulting in to saturation current.

From the semi-log graph (Fig 6.4), we can still discuss some properties of the sample. By extrapolating the straight line portion of the curve ln (J) Vs V for small

positive voltage, usually very close to $V = 0V$, one can determine the value for the reverse saturation current.

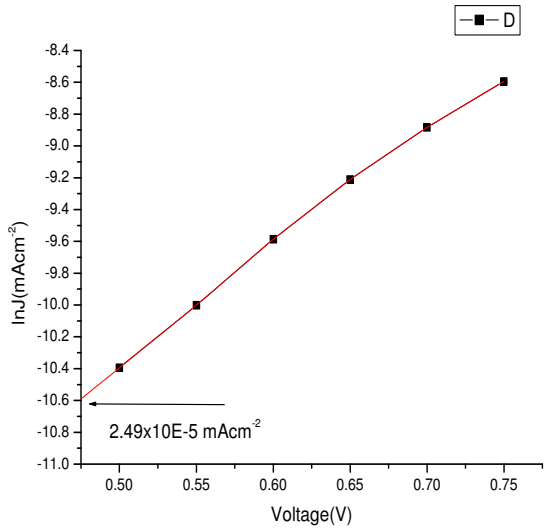

Figure 6.5: Semi logarithmic scale in dark

So, from the graph, the reverse saturation current density is determined to be about $2.49 \times 10^{-5} mAcm^{-2}$. This J_o is small ($\sim 10^{-8} mAcm^{-2}$) compared with the current density of the experimental interest, the contact will effectively block current flow for one sign of the applied voltage (reverse bias).

Once J_o is found, the barrier height per unit charge can be determined using the relation $\phi_b = \frac{kT}{q} ln(\frac{A^* T^2}{Jo})$.

$$\text{where, } \frac{K}{q} = 8.62x10^{-5}, T = 298K, A^* = 120 \frac{A}{cm^2 K^2} ,$$

The barrier height is found to be 0.86 eV. Again using the $(\frac{\triangle lnJ}{\triangle V})$ slope of the graph, one can calculate the diode ideality factor or quality factor n using the relation

$$n = \frac{q}{KT(\frac{\partial \ln J}{\partial V})}$$

The diode ideality factor is calculated to be 2.88. For ideal diode case, an increase in n requires an increase in J_o. If, n is 1, J_o only consists of recombination current. but, if n is greater than 1, then J_o also includes a recombination component from the junction[23]. Generally, $n \simeq 2$ but, for organic solar cells it is usually in the range of 2 upto 3[24]. Our DUT is in good agreement with this hypothesis.

6.3 J-V characteristics under illumination

Figure 6.4 shows the J-V curve of our sample under illumination of white light with intensity $2.5m\frac{W}{m^2}$.

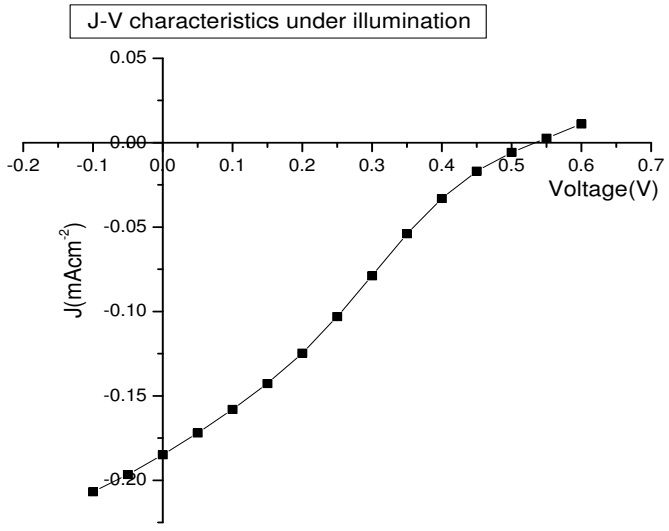

Figure 6.6: J-V curve under illumination

So, under open circuit conditions electrons are transported to the LUMO of the PCBM while holes are transported to the HOMO of MDMO:PPV (holes

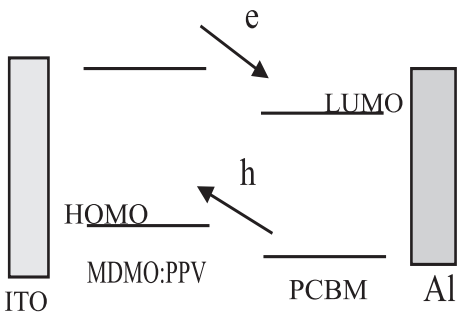

Figure 6.7: open circuit condition

move against a potential gradient while electrons move down the slope along the potential gradient). When a forward bias voltage is applied, since the work function of LUMO of the PCBM (3.7 eV)[25] is less than the work function of Aluminium ($4.28eV$), electrons are collected by the Aluminium while the holes facilitated by PEDOT:PSS are collected through the ITO .

From the J-V characteristic curve, a fill factor of 0.26, open circuit voltage 534 mV, short circuit current density 0.185 mAcm^{-2} and power conversion efficiency of 1.03% were obtained. Previous research works have shown that MDMO:PPV blended with PCBM, have power conversion efficiencies upto 2.8%[26]. Efficiency is affected by J_{sc}, V_{oc} and FF in addition to device structure and material properties. J_{sc} is affected by generation and dissociation rates of excited states as well as mobility of free charge carriers. In bulk heterojunction films, the exciton dissociation rate is efficient due to an immediate interface between donor and acceptor molecules. The optical absorption of most polymers covers only the visible range of the solar spectrum. This leads to a decrement in the power conversion efficiency because, a substantial solar energy is located in the red and infrared region. This problem can be avoided if we have thick films. But, making thick films increases the probability of recombination of charge carriers. The obtained FF is very low which can be attributed to poor transport property of the sample. The effect of V_{oc} is discussed

under section 6.5

6.4 Dependence of photocurrent on the incident light intensity

The basic aim of this study is to investigate the relationship between the photovoltaic parameters and the light intensity incident on the solar cell which is made from MDMO;PPV blended with PCBM in 1:4 weight ratio. For this purpose we have used various intensities ranging from $1-7.5\ mWcm^{-2}$. As it can be seen clearly in figure 6.8, the short circuit current decreases with increasing light intensity.

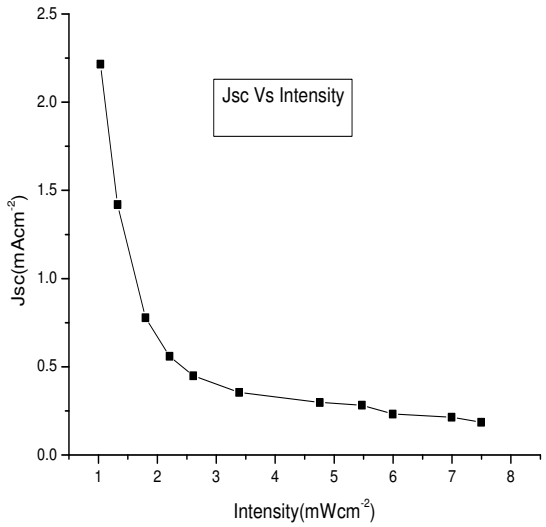

Figure 6.8: Dependence of short circuit current on the incident light intensity

It appeared in the graph that J_{sc} is not proportional to intensity. For this particular polymer blend type, the photocurrent is found to be decreasing for high amount of intensities. MDMO:PPV blended with PCBM is very sensitive to variation

of light intensity. The given polymer type has large bulk resistivity specially at high photon densities[24]. So, this bulk resistance decreases the photocurrent when the sample is shined with increased amount of intensity. Initially, the short circuit current drastically decreases with intensity upto $2.5mWcm^{-2}$. Further, increase on intensity induces only small change on the photocurrent and then J_{sc} appeared to be saturated at the value $0.25mAcm^{-2}$. In general MDMO:PPV blended with PCBM is very sensitive to variation of intensity and large photocurrent can be obtained for intensities as low as a fluorescent light for bias voltage ranging from $-2to+2v$.

In addition, the dependence of Jsh on the effective voltage $(Voc-Va)$[27] is responsible for the difference in the short circuit current density. From the above relation as the intensity is increased, the photocurrent is found to be decreasing. This is because, increasing the light intensity without changing the effective applied voltage $(Voc-Va)$ will not change the rate at which the excitons will be dissociated into free charge carriers (in this experiment the applied voltage was kept constant for the continuously varying intensity). As the intensity increases, there will be an extremely large number of excitons and hence, if there is no high enough effective applied voltage that dissociates the excitons into free charge carriers, it leads to a high probability of recombination which doesn't contribute to the photocurrent. When light intensity is increased, the space-charge limited regime grows and extends to higher $Vo-Va$ [28].

6.5 Dependence of open circuit voltage on the incident light intensity

When the photocurrent was measured with different intensities (as mentioned in section 6.4), the open circuit voltage was simultaneously measured. The following figure shows the variation of the open circuit voltage with the incident light intensity.

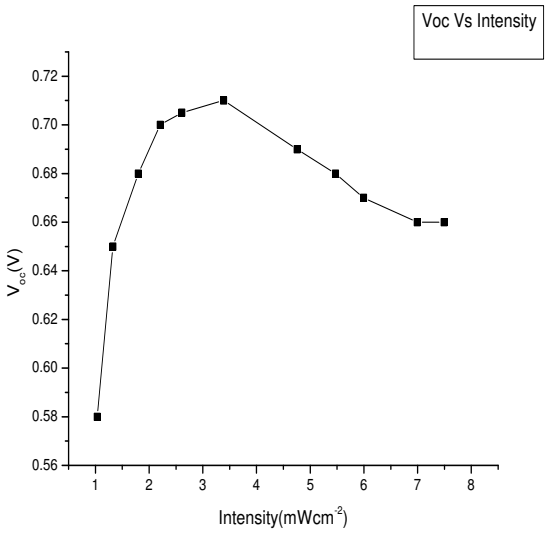

Figure 6.9: Dependence of open circuit voltage on the incident light intensity

The open-circuit voltage mainly originates from the electronic levels of the donor polymer and the acceptor molecule. In general V_{oc} is limited by several factors including interfacial energy levels, shunt losses, interfacial dipoles and morphology of the active film. Thus, the origin of V_{oc} in bulk heterojunctions is not well defined[22]. Previous works have revealed that V_{oc} (for single layered) devices mainly depends on the work function difference between the two electrodes. Also it has been shown that V_{oc} is affected by the morphology of the active layer and variations in the electron -acceptor strength [29]. V_{oc} is not entirely change in the work function difference of the two electrodes. Because, there is ground state dipole formation at the polymer-metal (or indeed the polymer-polymer) interface and also from the theoretical part discussed under section 4.2, it is highly dependent on the temperature.

Clearly, from figure 6.9, there are two distinct regions. The first region is characterized by a sharp increment of the photo voltage. In this region, the

intensity increment leads to an intensity dependent open-circuit voltage. At V_{oc}, the diffusion current has to cancel the drift current. This is possible due to the increment of the intensity for the first part of the graph. But for high values of the intensity, the contribution of the intensity to V_{oc} is reduced and hence, the V_{oc} is found to be inversely related with the intensity.

6.6 Impedance Spectroscopy

Figure 6.10 shows the impedance spectroscopy of our sample as a function of frequency and bias voltage. The scattered points are the measured coordinates of the real and imaginary parts of the impedance of the device under test. As it can be clearly seen from the graph, the impedance spectra consists of a portion of a single semicircle whose diameter corresponds to the resistance of the depletion layer for the respective bias voltages. These semicircles are bias dependent. The smaller bias voltages give a larger diameter which is to mean that, the resistance of the sample is larger at small voltages and can prevent large current flow. This is consistent with the J-V characteristics.

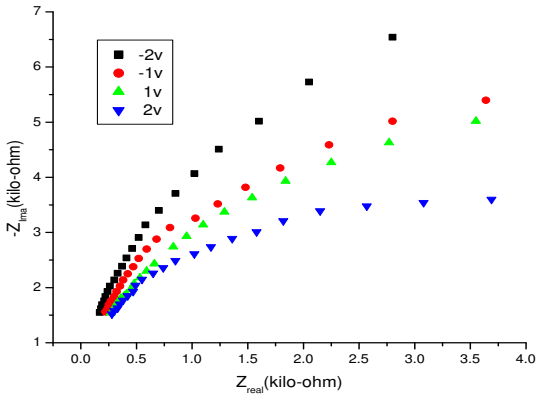

Figure 6.10: Cole-Cole plot of our sample

From the work functions of the polymers, it is expected that the work function of PEDOT:PSS [$\phi_{PEDOT:PSS} = 5.2eV$][30] and HOMO of MDMO:PPV [$\phi_{HOMO} = 5.3 \pm 0.1eV$][31] form an ohmic contact for hole injection into the HOMO level of MDMO:PPV. But, the work function of Aluminium ($4.28eV$)[12] doesn't match the LUMO level of the PCBM (3.7eV)[25], which result in an interface potential barrier of $\phi_b = 0.87$eV.

An ideal Cole-Cole plot of the complex impedance is a semicircle with its center on the real axis. Furthermore, the zero and the infinite frequency intercept on the Z_{real} axis[33]. This semicircle agrees with the model where a single barrier at the Al - polymer blend interface. There is no evidence for partially or completely overlapping second semi-circle due to a barrier at the other electrode. Normally, the zero frequency real impedance is obtained by extrapolating. The contact resistance (R_c), is the distance from the origin to the intersection of the semicircle with the real axis of the impedance plot that corresponds to the highest frequency. The relation $-Z_{imag} = (\omega c)^{-1}$ is used to estimate the value of the capacitance C. The parameters from the Cole-Cole plot are listed in Table 6.1

V_b(V)	$R_c(\Omega)$	$R(k\Omega)$	$C(nFcm^{-2})$
-2	186	13.1	2.4
-1	186	11.78	2.7
1	186	9.94	3.2
2	186	7.22	4.4

Conclusion

In this work, the light dependence of short circuit current and open circuit voltage were investigated using bulk-heterojunction solar cell. The study was carried out based on the J-V characteristics under dark and illumination as well as complex impedance measurement of the sandwich structure ITO | MDMO:PPV-PCBM | Al. The energy band gap of MDMO:PPV was estimated to be $2eV$ from the optical absorption spectrum. And the maximum absorption for pure and blend polymer took place at about a wave length of 500 nm. The dark J-V curve of our device manifests the properties of trap controlled space charge limited current. But, for low voltages the current is ohmic, and also a rectification ratio of 157 was obtained. In the J-V measurement under illumination, a fill factor of 0.26, open circuit voltage 534 mv, short circuit current density 0.185 mAcm^{-2} and power conversion efficiency of 1.03% were obtained. In the investigation of intensity dependence of J_{sc}, it was found that, at constant bias voltage, the J_{sc} decreases until it gets a value where J_{sc} saturates. Whereas the open circuit voltage manifests different properties for different intensities. From the complex impedance spectroscopy, it was possible to obtain a contact resistance of 186Ω and the different values of bulk resistances are given in Table 6.1

Bibliography

[1] Rene Janssen, Absorbing infrared light in polymer solar cells, The international society for optical engineering, (2006).

[2] Seamus Curran, David Gutin and James Dewald, Cascade solar cell, The international society for optical engineering, (2006).

[3] Gordon G. Wallace, Paul C.Dastoor, David L.Officer, Chee.O. Too, Conjugated Polymers, Chemical Innovation, Vol **30**, No 1, 14-22 (2000).

[4] Tolessa Yadete, Photovoltaic Properties of PTOPT, Msc.Thsis, Addis Ababa Univeristy, (1998).

[5] Bantikassegn Workalemahu, Ph.D Dissertation, ISBN 91-7871-803-1, Linkoping University, Sweden, (1996).

[6] Genene Tessema, Polymer physics, Addis Ababa University, (2006).

[7] Jean-Pierre Farges, Organic Conductors, Marcel Dekker, Inc. (1994) London.

[8] Colin Pratt, Conducting Polymers, Kingston University London, (1996).

[9] Siegmar Roth, Hartmut Bleier, Wojciech Pukacki, Farad Discuss, Chem. Soc., **88**, 223-233, (1989).

[10] R.Zallel, The physics of Amorphous Solids, Newyork, John Willey & sons, (1983).

[11] N.F Mott, Conduction in Non-Crystalline materials, 2nd edition, Clarendon Press, Oxford, (1993).

[12] Donald A.Neamen, Semiconductor Physics and Devices, Richard D.Irwin, Inc., (1992).

[13] S.M.Sze, Physics of Semiconductor Devices, 2nd edition, John Wiley & Sons, Newyork, (1981).

[14] Wudyalew Tessema, Electrical properties of junctions between Aluminium and POPT, Msc.Thesis, Addis Ababa Univeristy, (1999).

[15] W.Bantikassegn & O.Inganas, J.Phys., **54** 2511 (1983).

[16] J.R. Macdonald, ed., Imedance Spectroscopy, Emphasizing Solid State Materials and Systems, John Wiley & Sons, Newyork, (1987).

[17] J.H. Burroughes, D.D. Bradley, A.R Brown, R.N. Marks, K.Mackay, R.H Friends, P.L. Burns and A.B Holmer, Nature, 347 (1990) 539. CRene Janssen, Absorbing infrared light in polymer solar cells, The international society for optical engineering, (2006).

[18] C.L. Braun, J.Chem.phys., **80** (1984),4157

[19] N.S.Sariciftci, L.Smil-Owitz, A.J. Heeger, F.Wudl, Science 258 (1992), 1474.P. Miles, Appl. Opt., **38** (1999) 566 -570.

[20] Dipl.Ing. Klaus Petritsch, Organic Solar Cell Architectures, Ph.D. Dissertation, Cambridge and Graz, (2000).

[21] Xiangjun Wang, Surface Energy Patterning and optoelectronic devices Based on Conjugated Polymers, Ph.D Dissertation, ISBN, Linkoping, Sweden, (2006).

[22] Abay Gadissa, Studies Of Charge Transport and Energy Level in Solar Cells Based on Polmer, Ph.D Dissertation, ISBN, Linkoping, Sweden, (2006).

[23] Jeffrey A. Mazer, Solar Cells, Kluwer Academic Publishers, Boston, (1997).

[24] Donald A. Seanor, Electrical Properties of Polymers, Academic Press, (1982).

[25] V.D Mihailetchi, P.W.M. Blom, J.C. Hummele and M.T. Rispens, J.Appl.Phys., Volume 94, Number 10, (2003)

[26] Rene' Janssen, Low band gap polymer Solar cells, Dutch Polymer Inistitute, (2006).

[27] V.D. Mihailetchi, L.J.A. Koster and P.W.M. Blom, J.Appl.Phy., **85**, 1782252, (2004)

[28] L.J.A. Koster, V.D. Mihailetchi, H.Xie and P.W.M.Blom, J.Appl.Phy., **87**, 203502 (2005).

[29] C.M. Ramsdale, J.A. Barker, A.C Arias, F.D. Mackenzie, R.H Fried, J.Appl.Phys.,**92** (2002).

[30] Andreas Petr, Fapei Zhang, Heiko Peisert, Martin Knupfer, Lothar Dunsch, Electro Chemical Adjustment of the Workfunction of Conducting Polymers, Highlights, (2003).

[31] D. Muhlbacher, H. Neugebauer, A. Cravino and N.S. Sariciftci, Mol.cryst, Liq.cryst, Vol **385**, 185-192 (2002).